Landau–Zener model for electron loss of low-energy negative fluorine ions to surface cations during grazing scattering on a LiF(001) surface*

Wang Zhou(周旺), Meixiao Zhang(张鹂枭), Lihua Zhou(周利华), Hu Zhou(周虎), Yulong Ma(马玉龙), Yanling Guo(郭艳玲), Lin Chen(陈林)†, and Ximeng Chen(陈熙萌)‡

School of Nuclear Science and Technology, Lanzhou University, Lanzhou 730000, *China*

(Received 16 January 2016; revised manuscript received 8 July 2016; published online 28 September 2016)

There is no available theoretical description of electron transfer from negative projectiles at a velocity below 0.1 a.u. during grazing scattering on insulating surfaces. In this low-velocity range, electron-capture and electron-loss processes coexist. For electron capture, the Demkov model has been successfully used to explain the velocity dependence of the negative-ion fraction formed from fast atoms during grazing scattering on insulating surfaces. For electron loss, we consider that an electron may be transferred from the formed ionic diabatic quasi-molecular state to the formed covalent diabatic quasi-molecular state by the crossing of the potential curves of negative projectiles approaching the surface cations, which can be described by the Landau–Zener two-energy-level crossing model. Combining these two models, we obtain good agreement between the experimental and calculated data for the F^-–LiF(001) collision system, which is briefly discussed.

Keywords: charge transfer, negative ion, grazing scattering, ionic crystal

PACS: 34.35.+a, 78.55.Fv, 79.20.Rf **DOI:** 10.1088/1674-1056/25/11/113401

1. Introduction

Electron transfer during particle–surface interactions has long been studied because it is closely related to reactive events and catalytic processes at surfaces. From an application perspective, electron transfer between particles and surfaces can be used to determine the elemental composition of a surface layer; i.e., the low-energy ion-scattering (LEIS) technique.

To further illustrate the importance of electron-transfer phenomena at surfaces, let us consider the scattering of atomic particles from insulator surfaces. Souda *et al.*[1–3] studied the target electronic excitation in low-energy H^+ (D^+) ions scattering from various ionic-compound surfaces, such as alkali-metal halides and oxides. The resonant tunneling process and energy-level crossing play important roles in the neutralization of H^+ ions, whereas the electronic excitation of surfaces is ascribed to the electron-promotion mechanism. Band effects on the neutralization of D^+ were later reported by Souda *et al.*[4] In particular, Winter *et al.*[5] first described high negative-ion formation for oxygen atoms during grazing scattering from a LiF(100) surface. One year later, Esaulov *et al.*[6] reported a dramatic increase in H^- formation in H^+ ion scattering on oxidized Mg and Al surfaces. Subsequently, these authors observed the efficient generation of a high negative-ion fraction when scattering on a MgO(100) crystal surface.[7] In 2011, Winter *et al.*[8] also investigated the H^- fraction on an oxidized NiAl(110) surface and found that the H^- fraction was nearly one order of magnitude smaller than that on a LiF(001) surface. It was concluded for both alkali-metal halide and oxide surfaces that the wide band-gaps strongly suppress the electron loss from the formed negative ion back to the ionic surface, resulting in a high negative-ion fraction. However, electron-loss processes related to the high survival of negative ions have not received as much experimental or theoretical attention as electron-capture processes.[7,9–12]

Theoretically, the concept of resonant electron transfer is not appropriate for insulator surfaces with wide band-gaps because the energy-level down shift is small given the image potential effect, Borisov *et al.*[13,14] proposed that the large energy-level difference between a projectile's affinity level and the valence band state of a surface can be significantly reduced by the Madelung potential of an ionic surface, which facilitates quasi-resonant electron capture. Based on this concept, the Demkov model[15,16] has been successfully applied to describe the electron-capture probability for negative-ion formation from the active anion site on insulator surfaces at small velocities above the velocity threshold of negative-ion formation (~ 0.1 a.u.). However, this model does not reproduce the experimental data at relatively high (≥ 0.3 a.u.) or low ($v \leq 0.1$ a.u.) velocities. The electron-loss process occurs and has been experimentally observed,[4] but it is not considered in the theoretical model. Recently, some efforts have been devoted to investigating relatively high velocities (≥ 0.3 a.u.), for which the electron tunneling in the repul-

*Project supported by the National Natural Science Foundation of China (Grant Nos. 11175075, 11405078, 11474140, 11404152, and 11305083).

†Corresponding author. E-mail: chenlin@lzu.edu.cn

‡Corresponding author. E-mail: chenxm@lzu.edu.cn

© 2016 Chinese Physical Society and IOP Publishing Ltd

sive Coulomb field built by both the formed negative ion and the anion site has been considered.[17] However, a quantitative agreement between experiment and theory without adjustable parameters has not yet been achieved, although several different mechanisms[18] have been proposed to qualitatively explain the experimental findings. In contrast, to our knowledge, no explanation has been developed for electron loss at very low velocities ($v \leq 0.1$ a.u.), it occurs efficiently on the ionic-surfaces (such as, MgO(100)[7] and LiF(001)[19]). Thus, understanding electron loss at very low velocities is urgently needed.

In this paper, we theoretically calculate the velocity dependence of the negative-ion fraction of negative fluorine ions scattering on a LiF(001) surface with a grazing incident angle of $\sim 1^\circ$ in the low-velocity range of $v \leq 0.1$ a.u. In this range, electron loss, which occurs efficiently at the cation sites of the LiF(001) surface, has been considered to be the main charge-transfer process. We use atomic units throughout this paper, unless otherwise specified.

2. Theoretical model and formulation

Before discussing electron loss at cation sites, let us first consider an atom colliding with anion sites on the insulator surface. These anions are regarded as active sites. When the atom approaches the active site, its affinity level decreases significantly because of the Madelung potential effect.[7] The energy defect ΔE_C between the affinity level and the valence band state of the surface can be approximated by the following equation:[11,13]

$$\Delta E_C(\boldsymbol{R}) \approx \Delta\varepsilon^{\text{binding}} + E_{\text{Mad}} - \frac{1}{R} + \Delta P(\boldsymbol{R}), \tag{1}$$

where $\Delta\varepsilon^{\text{binding}}$ represents the binding-energy difference between the final states; E_{Mad} is the Madelung potential shift, which is equal to 12.5 eV;[20] and R represents the distance between the projectile and the active site. $\Delta P(\boldsymbol{R})$ is the polarization effect, which includes the polarization of the scattered negative ion by the +1 charge at the halide hole on the surface, and vice versa, and the interaction of the negative ion with its image charge and the Mott–Littleton contribution from the halide hole.[20]

For simplicity, we neglect the first two polarization effects and take into account only the Mott–Littleton contribution. The projectile captures an electron from the anion site and leaves a hole at the site. This electron–hole pair creates the resulting electric dipole moment $e\boldsymbol{R}$ that polarizes the lattice ions. The corresponding correction term, named the Mott–Littleton interaction, for the final energy of the system is given by

$$\Delta P(\boldsymbol{R}) = E_{\text{ML}}(\boldsymbol{R}) = -\frac{1}{2}\sum_k \alpha_k \left(\frac{\boldsymbol{R}_k}{R_k^3} - \frac{\boldsymbol{R}_k - \boldsymbol{R}}{|\boldsymbol{R}_k - \boldsymbol{R}|^3}\right)^2,$$

where k runs over all lattice sites $\boldsymbol{R}_k$ except the active one, and the polarization α_k for LiF(100) ($\alpha_{\text{Li}^+} = 0.029$ A^3, $\alpha_{\text{F}^-} = 0.644/0.759$ A^3) is taken from Ref. [21] and is smaller than that for an MgO crystal ($\alpha_{\text{Mg}^{2+}} = 0.0955$ A^3, $\alpha_{\text{O}^{2-}} = 1.6473$ A^3).[21–23] From Refs. [22] and [23], we also obtain the lattice constants $a_{\text{LiF}} = 7.6$ a.u. for LiF and $a_{\text{MgO}} = 7.9554$ a.u. for MgO. Moreover, for F^0–MgO(100), the reduction of the Mott–Littleton interaction by the energy defect is of the order of 0.5 eV in the interaction region.[22] For the F^0–LiF(001) system, we simply take the upper limit value of $\Delta P(\boldsymbol{R}) = -0.5$ eV. In general, ΔE_C is almost constant for a small R.[24] If we assume that R_{eff} is the distance for which charge transfer occurs more efficiently along the projectile's trajectory, then equation (1) can be replaced by $\Delta E_C \approx \Delta\varepsilon^{\text{binding}} + E_{\text{Mad}} - \frac{1}{R_{\text{eff}}} + \Delta P(R_{\text{eff}})$, where $R_{\text{eff}} = 2.5$ a.u. and $\Delta\varepsilon^{\text{binding}} = 0$.[25] Finally, we obtain $\Delta E_C \approx 1.12$ eV at R_{eff}.

Negative-ion formation via electron transfer from the anion site to the atomic projectile occurs efficiently, and the electron-capture probability P_{cap} is described by the Demkov model[15,16,24,26]

$$P_{\text{cap}}(v, \Delta E_C) = \frac{1}{2}\,\text{sech}^2\left[\frac{\pi\left(\Delta E_C + v^2/2\right)}{2\gamma v}\right], \tag{2}$$

where $\gamma = \left(\sqrt{2E_t} + \sqrt{2E_p}\right)/2$, v is the incident velocity, and E_t and E_p are the ionization potentials of the target and the projectile, respectively. This model successfully describes the rapid increase in the negative-ion fraction with increasing parallel velocity near the velocity threshold of 0.1 a.u.

In our previous study,[17] we introduced electron-tunneling behavior to describe the destruction of formed negative ions at surface anions. For a grazing incident angle of $\sim 1^\circ$, the motion of a projectile along the surface plane can be decoupled into parallel and perpendicular motions. As the projectile approaches the surface, the formed negative ion can be destroyed via quantum tunneling of electrons in the repulsive Coulomb field built by both the negative ion and the anion site. Thus, the electron-loss probability is calculated using the Wentzel–Kramers–Brillouin (WKB) barrier penetration probability within the action integral, which is given by[27]

$$P_{\text{tunneling}}(E_\perp) = \exp\left[-2\int_{r_1}^{r_2}\sqrt{2\left(V(r) - E_\perp\right)}\,\mathrm{d}r\right], \tag{3}$$

where $V(r) = 1/r$ for alkali halides, the lower limit of integration $r_1 = \frac{1}{E_\perp + I}$,[28] the turning point of classical orbits $r_2 = 1/E_\perp$, the perpendicular energy $E_\perp = \frac{1}{2}M(v\sin\alpha)^2$, I is the projectile electron affinity energy, M is the projectile atomic mass, and α is the incident angle with respect to the surface plane. Clearly, $P_{\text{tunneling}}$ decreases as the projectile velocity v decreases, as shown by the solid green line in Fig. 2, i.e., for $v = 0.1$ a.u., $P_{\text{tunneling}} = 0.0014$. Therefore, the electron-loss channel via this mechanism can be neglected

when v is less than 0.1 a.u. According to Ref. [29], kinetically assisted resonant tunneling to the conduction band bottom of the LiF surface requires a high projectile velocity, exceeding 0.173 a.u.; thus, it is also unlikely to occur in our present velocity range.

However, the projectile collides not only with the anion sites of the ionic surface but also with the cations. Now, we discuss a series of soft binary collisions between a negative projectile ion and the cation sites where electron transfer may occur as follows:

$$\mathrm{Li}^{+}_{\mathrm{active}} + \mathrm{F}^{-} \rightarrow \mathrm{Li}^{0}_{\mathrm{active}} + \mathrm{F}^{0}. \tag{4}$$

Based on the energy-conservation requirement, we can simply analyze the electron-transfer process. The conduction band of bulk LiF consists of the 2s, 2p states of Li, and the 3d state of F.[30] According to Refs. [31] and [32], the first-empty band corresponds to a Li^{+} ion 2s electron and to the conduction band bottom energy level of the LiF(001) surface. This can be simply understood in terms of the shift of the 2s energy level of the free Li atom from -5.4 eV to approximately 2.0 eV[22,23] via the Madelung potential and correlation and exchange effects.[33,34] From Eq. (4), we obtain the initial energy

$$\begin{aligned} & E\left(\mathrm{Li}^{+}_{\mathrm{active}} + \mathrm{F}^{-}\right) \\ = {} & E_{\mathrm{Li}^{+}} + E_{\mathrm{F}^{-}} + \frac{1}{2}\sum_{i\neq j}\frac{q_i q_j}{|\boldsymbol{r}_i - \boldsymbol{r}_j|} \\ & + \sum_i \frac{q_i}{|\boldsymbol{r}_i|} - \sum_i \frac{q_i}{|\boldsymbol{R} - \boldsymbol{r}_i|} - \frac{1}{|\boldsymbol{R}|} + P_{\mathrm{initial}}(\boldsymbol{R}), \end{aligned} \tag{5}$$

where $E_{\mathrm{Li}^{+}}$ and $E_{\mathrm{F}^{-}}$ are the total energies of the free Li^{+} ion and the projectile F^{-}, respectively. $q_i = \pm 1$ represents the point charges at the crystal sites located at r_i relative to the active site. The third term gives the interaction energy between the point charges of the crystal, excluding the active site. The fourth term is the interaction energy between the active site (having a charge of $+1$) and all other sites of the crystal. The fifth term is the interaction energy between the projectile and the point charges without the active site. The sixth term is the interaction energy between the projectile and the active site. The last term is the polarization interaction energy of the negative projectile for the whole LiF target.

Similar to the initial state, we obtain the energy of the final state as follows:

$$E\left(\mathrm{Li}^{0}_{\mathrm{active}} + \mathrm{F}^{0}\right) = E_{\mathrm{Li}^{0}} + E_{\mathrm{F}^{0}} + \frac{1}{2}\sum_{i\neq j}\frac{q_i q_j}{|\boldsymbol{r}_i - \boldsymbol{r}_j|} + P_{\mathrm{final}}, \tag{6}$$

where the last term P_{final} represents the Mott–Littleton polarization interaction energy, which includes the polarization interaction energy of the extra electron for the active Li^{+} ion $P_{\mathrm{Li}^{+}_{\mathrm{active}}+\mathrm{e}}$ and all other sites of the crystal. References [33] and [34] noted that for a hole in a LiF crystal, this energy is 2.644 eV; therefore, for an extra electron on the Li^{+} ion site in the final state, the corresponding Mott–Littleton polarization interaction energy is $P_{\mathrm{final}} = -2.644$ eV. Additionally, according to Ref. [20], considering the short-range correlation effect of the polarization of the central-cell ion by an extra electron at the Li^{+}-ion site, we can reasonably assume that the electron is largely localized and, thus, the polarization correction is $P_{\mathrm{Li}^{+}_{\mathrm{active}}+\mathrm{e}} \approx -1.0$ eV. Therefore, the total polarization interaction energy of the extra electron at other crystal sites is approximately -1.644 eV, except for the active site of the Li^{+} ion.

From Eqs. (5) and (6), we obtain the energy difference between the final and initial states; i.e.,

$$\begin{aligned} \Delta E_{\mathrm{L}}(\boldsymbol{R}) &= E\left(\mathrm{Li}^{0}_{\mathrm{active}} + \mathrm{F}^{0}\right) - E\left(\mathrm{Li}^{+}_{\mathrm{active}} + \mathrm{F}^{-}\right) \\ &= \varepsilon_{\mathrm{Li}^{0}} + \varepsilon_{\mathrm{F}^{-}} - \sum_i \frac{q_i}{|\boldsymbol{r}_i|} + \sum_i \frac{q_i}{|\boldsymbol{R} - \boldsymbol{r}_i|} + \frac{1}{R} + \Delta P', \end{aligned} \tag{7}$$

where $\varepsilon_{\mathrm{Li}^{0}} = E_{\mathrm{Li}^{0}} - E_{\mathrm{Li}^{+}} = -5.4$ eV[33,34] and $\varepsilon_{\mathrm{F}^{-}} = E_{\mathrm{F}^{0}} - E_{\mathrm{F}^{-}} = 3.4$ eV.[24] The third term gives the Madelung potential created by the point charges at the Li^{+} site ($E_{\mathrm{Mad}}(\boldsymbol{R}=0) \equiv E_{\mathrm{Mad}} = 12.5$ eV[33,34]). Thus, it is reasonable to take $\sum_i \frac{q_i}{|\boldsymbol{R}-\boldsymbol{r}_i|} \approx 0\,(R \equiv |\boldsymbol{R}|)$. The last term, $\Delta P' = P_{\mathrm{final}} - P_{\mathrm{initial}}$, is the polarization correction of the energy difference. For simplicity, we neglect the initial F^{-} projectiles' polarizations for the whole LiF crystal and only consider the Mott–Littleton polarization interaction of the extra electron for the whole LiF crystal in the final state. Thus, $\Delta P' \approx P_{\mathrm{final}} = -2.644$ eV. Finally, equation (7) can be rewritten as

$$\Delta E_{\mathrm{L}}(\boldsymbol{R}) = \varepsilon_{\mathrm{Li}^{0}} + \varepsilon_{\mathrm{F}^{-}} - E_{\mathrm{Mad}} + \frac{1}{R} + \Delta P'. \tag{8}$$

Equation (8) gives the distance-dependent energy defect, which can be used for the short ion surface distance. From Eq. (8), we can easily see that $R_{\mathrm{c}} = -1/(\varepsilon_{\mathrm{Li}^{0}} + \varepsilon_{\mathrm{F}^{-}} + \Delta P' - E_{\mathrm{Mad}}) = 1.6$ a.u., where the energy defect ΔE_{L} is equal to zero. This value corresponds to the crossing of the potential curves. In Fig. 1, for large $R > R_{\mathrm{c}}$ (region I), $\Delta E_{\mathrm{L}}(\boldsymbol{R}) < 0$; therefore, the reaction in Eq. (4) may be exothermic. However, according to the previous theoretical studies of the thermal energy of ion–ion collisions,[35–37] radiative charge transfer is the main mechanism at energies of less than 1.4 eV, and the corresponding cross section is of the order of 10^{-19}–10^{-23} cm^2.[38,39] This cross section is too small to occur here, where the perpendicular energy is in the same range. Therefore, electron loss mainly occurs near the range $R \leq R_{\mathrm{c}}$ (region II).

According to Ref. [40], if R is less than a critical distance $(13.6/\varepsilon_{\mathrm{F}^{-}})^{1/2} = 2$ a.u., the description of the atomic distribution of electrons becomes invalid. Instead, a molecular characterization must be adopted for the single-electron

transition between collision partners. Therefore, equation (4) can be regarded as describing an electron transferring from the formed ionic diabatic quasi-molecular state $\left(\mathrm{Li}^{+}_{\mathrm{active}}(2\mathrm{s})+\mathrm{F}^{-}\right)$ to the formed covalent diabatic quasi-molecular state $\left(\mathrm{Li}^{0}_{\mathrm{active}}(2\mathrm{s})+\mathrm{F}^{0}\right)$ as a result of the potential energy levels crossing because of the ionic-covalent configuration interaction during the collision process.

Based on this physical picture, two energy levels crossing according to the Landau–Zener model may be appropriate. The requirements for the Landau–Zener model are as follows.

(i) The Landau–Zener model requires that the energy separation of the reactants and the products at infinite internuclear separations is large.[41]

(ii) The energy of relative motion at the crossing is substantially greater than the difference between the exact Eigenenergies there, as encountered for $E_{\mathrm{p}} \gg 2\left|V_{\mathrm{transfer}}(R_{\mathrm{c}})\right|$.[42]

(iii) Zener's initial derivation of his model[43] requires $V_{\mathrm{transfer}}(R)$ to be constant for all time. However, in reality, according to the subsequent analysis of Bates,[42] this transition occurs appreciably only in a very narrow zone around the crossing; hence, $V_{\mathrm{transfer}}(R)$ needs to be constant only in this zone.

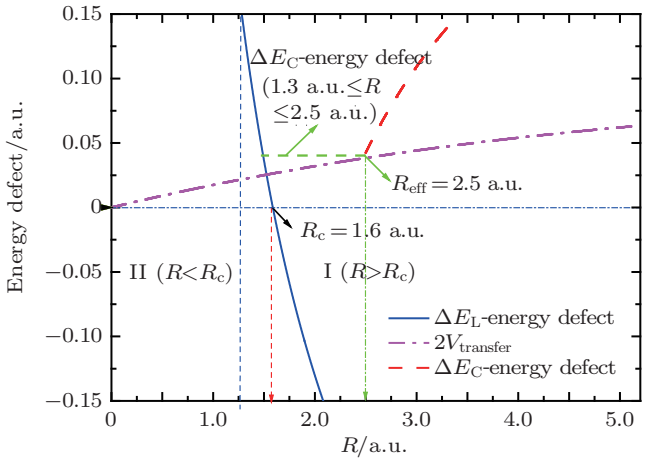


Fig. 1. (color online) The energy defect ΔE_{L} (solid blue line), ΔE_{C} (dashed red line), and $2V_{\mathrm{transfer}}$ (dashed/dotted magenta line) as a function of distance R. The dotted green line shows the constant energy defect ΔE_{C} for a small R in the range of 1.3 a.u. $\leq R \leq$ 2.5 a.u. (details in text).

Here, $2V_{\mathrm{transfer}}(R_{\mathrm{c}}) = 0.026$ a.u. (0.7075 eV) is small relative to most of our projectile energy range. Figure 1 shows the very slow increase in $2V_{\mathrm{transfer}}(R)$ with R near the crossing point R_{c}. Thus, the above-mentioned requirements are well satisfied.

The well-known Landau–Zener model for a two-state energy level crossing[44,45] describes the electron-loss process between the ionic diabatic quasi-molecular state $\left(\mathrm{Li}^{+}_{\mathrm{active}}(2\mathrm{s})+\mathrm{F}^{-}\right)$ energy level and the covalent diabatic quasi-molecular state $\left(\mathrm{Li}^{0}_{\mathrm{active}}(2\mathrm{s})+\mathrm{F}^{0}\right)$ energy level with a transition probability which is expressed as[44,45]

$$P_{\mathrm{LZ}} = 1-\exp\left[-\frac{2\pi\left|V_{\mathrm{transfer}}(R_{\mathrm{c}})\right|^{2}}{\left|\Delta E'_{\mathrm{L}}(R_{\mathrm{c}})\right| v_{\mathrm{eff}}}\right] = 1-\exp\left(-\frac{\beta_{\mathrm{L}}}{v_{\mathrm{eff}}}\right). \quad (9)$$

In a diabatic representation,

$$\beta_{\mathrm{L}} = 2\pi\left|V_{\mathrm{transfer}}(R_{\mathrm{c}})\right|^{2}/\left|\Delta E'_{\mathrm{L}}(R_{\mathrm{c}})\right|,$$

where $V_{\mathrm{transfer}}(R_{\mathrm{c}})$ denotes the electron-transfer interaction matrix elements of these two diabatic quasi-molecular energy levels at a crossing point R_{c}.

$$\Delta E'_{\mathrm{L}}(R_{\mathrm{c}}) = \frac{\mathrm{d}\Delta E_{\mathrm{L}}(R)}{\mathrm{d}R}\Big|_{R=R_{\mathrm{c}}} = -\frac{1}{R_{\mathrm{c}}^{2}}$$

is the difference between the diabatic quasi-molecular potential curve slopes at the crossing point R_{c}, where $\Delta E_{\mathrm{L}}(R)$ is the energy difference between the two interaction diabatic quasi-molecular energy levels given by Eq. (8). Therefore, $\Delta E'_{\mathrm{L}}(R)$ actually reflects the difference in "force" acting upon the two diabatic quasi-molecular states.[44,45]

According to Ref. [46], the diabatic representation allows one to calculate the ionic adiabatic quasi-molecular potential $E^{\mathrm{adiabatic}}_{\mathrm{initial}}\left(\mathrm{F}^{-}+\mathrm{Li}^{+}_{\mathrm{active}}(2\mathrm{s})\right)$ and covalent adiabatic quasi-molecular potential $E^{\mathrm{adiabatic}}_{\mathrm{final}}\left(\mathrm{F}^{0}+\mathrm{Li}^{0}_{\mathrm{active}}(2\mathrm{s})\right)$ of the ionic diabatic quasi-molecular state and the covalent diabatic quasi-molecular state, as well as their splitting $\Delta E^{\mathrm{adiabatic}}(R)$. In the two-state case,

$$\begin{aligned}&\Delta E^{\mathrm{adiabatic}}(R)\\ &= \left\{\left[E\left(\mathrm{F}^{-}+\mathrm{Li}^{+}_{\mathrm{active}}(2\mathrm{s})\right)\right.\right.\\ &\quad \left.\left.-E(\mathrm{F}^{0}+\mathrm{Li}^{0}_{\mathrm{active}}(2\mathrm{s}))\right]^{2}+4V^{2}_{\mathrm{transfer}}(R)\right\}^{1/2}.\end{aligned}$$

In the Landau–Zener model, this obviously leads to $\Delta E^{\mathrm{adiabatic}}(R_{\mathrm{c}}) = 2V_{\mathrm{transfer}}(R_{\mathrm{c}})$, which corresponds to the minimum of the adiabatic splitting $\Delta E^{\mathrm{adiabatic}}(R)$ and represents the non-crossing of the ionic adiabatic quasi-molecular potential by the covalent adiabatic quasi-molecular potential. Additionally, it should be noted that R_{c} actually reflects the center of the non-adiabatic region in an adiabatic representation.

For a single-electron transition, the semi-empirical formula given in Refs. [40] and [46] is used in the present work for the charge-transfer matrix element $V_{\mathrm{transfer}}(R) = \varepsilon^{1/2}_{\mathrm{F}^{-}}\varepsilon'^{1/2}_{\mathrm{Li}^{0}(2\mathrm{s})}R^{*}\mathrm{e}^{-0.86R^{*}}$ with $R^{*} = (\sqrt{2\varepsilon_{\mathrm{F}^{-}}}+\sqrt{2\varepsilon'_{\mathrm{Li}^{0}(2\mathrm{s})}})R/2$ between an ionic state and a covalent state, where $\varepsilon_{\mathrm{F}^{-}} = 3.4$ eV and $\varepsilon'_{\mathrm{Li}^{0}(2\mathrm{s})} = 2.0$ eV.[22,23] We then obtain $\beta_{\mathrm{L}} = 0.0028$ a.u. This formula reflects the interaction between the initial ionic diabatic quasi-molecular state and the final covalent diabatic quasi-molecular state.

According to Ref. [42], the width ΔR of the transition zone is $(4\pi v_{\mathrm{eff}}\hbar s/\alpha)^{1/2}$, where $\alpha = e^{2}/R_{\mathrm{c}}^{2}$. $\Delta R = R_{\mathrm{c}}\left(4\pi\hbar s v_{\mathrm{eff}}/e^{2}\right)^{1/2} \approx 0.28R_{\mathrm{c}}s^{1/2}\left(E_{\perp}/M\right)^{1/4}$, where $E_{\perp}$ is in

units of eV, and M is the projectile mass and is presented using the chemical (^{16}O) scale because the Li^+ ion is fixed at the LiF crystal site. s is a dimensionless quantity that is somewhat greater than unity. Using the same treatment as that used by Bates *et al.*,[42] we replace $0.28s^{1/2}$ with 0.35 and obtain $\Delta R \leq 0.3$ a.u. in our energy range. Therefore, the charge transfer occurs only in a small region near the crossing point R_c. For simplicity, we keep the projectile velocity constant throughout the collision process and take the effective projectile velocity $v_{\text{eff}} = v_{\perp} = v\sin\alpha$.

For a single collision of the atom with the active anion site on the surface in the present velocity range, we obtain the single-collision, electron-capture probability along the incoming and outgoing trajectory of the projectile in the electron capture region; i.e.,

$$P_1 = 2P_{\text{cap}}\left(1-P_{\text{cap}}\right). \tag{10}$$

In contrast, for a single collision of the F^- ion with the Li^+ cation site, we obtain the electron-loss probability $P_{\text{LZ}}\left(1-P_{\text{LZ}}\right)P_{\uparrow}\left(1-P_{\downarrow}\right)+P_{\text{LZ}}\left(1-P_{\text{LZ}}\right)P_{\downarrow}\left(1-P_{\uparrow}\right)$ when the process occurs only along the incoming trajectory of the F^- projectile in the electron-loss region. However, if this process occurs only along the outgoing trajectory, the electron-loss probability is as follows: $\left(1-P_{\text{LZ}}\right)P_{\text{LZ}}P_{\uparrow}\left(1-P_{\downarrow}\right)+\left(1-P_{\text{LZ}}\right)P_{\text{LZ}}P_{\downarrow}\left(1-P_{\uparrow}\right)$, where $P_{\uparrow}=P_{\downarrow}=1/2$ represents the spin statistic. Consequently, the electron-loss probability throughout the trajectory is

$$P_2 = 4P_{\text{LZ}}\left(1-P_{\text{LZ}}\right)P_{\uparrow}\left(1-P_{\downarrow}\right). \tag{11}$$

Before moving away from the surface, the incoming negative ion experiences a series of collisions with the active anion and cation sites at a grazing incident angle of $\alpha = 1^\circ$. After N sequential effective collisions, the final negative-ion fraction $P(N)$ obeys the following first-order, linear, non-homogeneous differential equation

$$\frac{\mathrm{d}P(N)}{\mathrm{d}N} = \left(1-P(N)\right)P_1 - P(N)P_2, \tag{12}$$

where the initial condition $P(N=0)=1$. Combining Eqs. (10)–(12), we obtain the final negative-ion fraction

$$P(N) = \frac{P_1}{P_1+P_2} + \frac{P_2}{P_1+P_2}\exp\left[-\left(P_1+P_2\right)N\right]. \tag{13}$$

In Fig. 1, $\Delta E_{\text{C}}(R)$ decreases as the distance R decreases. Reference [24] noted that ΔE_{C} generally decreases to a constant value for small R. Therefore, when the distance is less than R_{eff}, $\Delta E_{\text{C}}(R)$ can be approximately replaced by a constant value of $\Delta E_{\text{C}}(R_{\text{eff}})$ in the effective R range of $R_m \leq R \leq R_{\text{eff}}$. $R_m = 1.3$ a.u. corresponds to a large energy defect $\Delta E_{\text{L}}(R) = 0.15$ a.u. (4.0 eV) where the electron loss occurs inefficiently. Moreover, based on the effective interaction length along the surface normal $d = R_{\text{eff}} - R_m \approx 1$ a.u., we obtain the effective number of binary collisions $N \approx 2d/\left(\frac{a_{\text{LiF}}}{2}\tan\alpha\right) = 30$ for the F^-–LiF(001) system.

3. Results and discussion

In Fig. 2, we display the calculated results for $F^{-/0}$ projectiles during grazing ($\alpha = 1^\circ$) scattering from the LiF(001) surface and the available experimental data.[19] For F^0 projectiles, the calculated results are presented from our previous study[17] for comparison. For F^- projectiles, The calculated results are in good agreement with the experimental data. For the F^- projectile incidence, the negative-ion fraction declines rapidly and then exhibits an inflection point. Subsequently, it increases slowly with velocity.

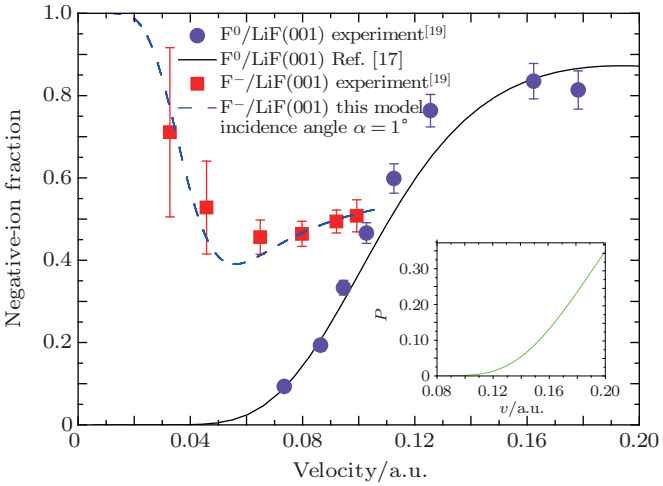


Fig. 2. (color online) Negative-ion fractions as a function of the incident velocity for $F^{-/0}$ projectiles during grazing ($\alpha = 1^\circ$) scattering from a LiF(001) surface. The data obtained for LiF(001) from Ref. [19]: F^-, solid red squares; F^0, solid violet circles. Theory: F^-, dashed blue line, this model; F^0, solid black line, Ref. [17]. The inset shows the electron-tunneling probability as a function of the projectile velocity for F^-/LiF(001) based on Eq. (3).

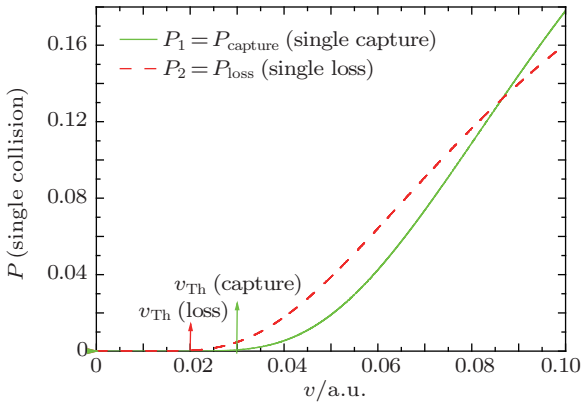


Fig. 3. (color online) The electron-capture and loss probabilities as a function of the incident velocity for a single collision with the LiF(001) surface active anion and cation sites during the trajectory, respectively. The solid green line represents the electron capture of a single collision with surface active anions, based on Eq. (10). The dashed red line indicates the electron loss of a single collision with surface active cations, based on Eq. (11). The green and red arrows indicate the electron-capture and loss velocity thresholds, respectively.

Figure 3 shows the electron-capture and loss probabilities for single collisions of the projectiles with active anion and cation sites on the LiF(001) surface. Clearly, the

velocity threshold of electron loss for the F^- projectile is $v_{\rm Th}^{\rm loss} = 0.02$ a.u. (indicated by the red arrow), which is slightly smaller than that of electron capture (0.03 a.u.). Moreover, the electron-loss probability is larger than the electron-capture probability when the velocity is below 0.09 a.u. Therefore, the negative-ion fraction initially decreases rapidly, as shown in Fig. 2.

To obtain the detailed variation tendency for the F^- ion fraction, we calculate $\mathrm{d}P(N=30,v)/\mathrm{d}v = 0$, where

$$\begin{aligned}&\frac{\mathrm{d}P(N,v)}{\mathrm{d}v}\\ &= \frac{P_1'P_2 - P_2'P_1}{(P_1+P_2)^2} + \frac{P_2'P_1 - P_2P_1'}{(P_1+P_2)^2}\exp\left[-(P_1+P_2)N\right]\\ &\quad - \frac{P_2}{P_1+P_2}N\left(P_1'+P_2'\right)\exp\left[-(P_1+P_2)N\right].\end{aligned}$$

This is a transcendental equation and cannot be solved analytically. However, it can be solved numerically. In Fig. 4, we show $\mathrm{d}P(N=30,v)/\mathrm{d}v$ as a function of the negative projectile velocity v (solid magenta line). Clearly, the solution of $\mathrm{d}P(N=30,v)/\mathrm{d}v = 0$ is $v_0 = 0.056$ a.u. For $v < 0.0362$ a.u., $\mathrm{d}P(N=30,v)/\mathrm{d}v < 0$ corresponds to the initial rapid decline in the negative F^- ion fraction in $0 < v < 0.0362$ a.u. in Fig. 2. 0.0362 a.u. $< v < v_0$ corresponds to the relatively slow decrease in the F^- ion fraction to its minimum (0.39) in this small velocity range. For $v > v_0$, $\mathrm{d}P(N=30,v)/\mathrm{d}v > 0$ and increases relatively slowly, which corresponds to the slow increase in the final negative-ion fraction after reaching its minimum.

According to Eq. (13), the asymptotic minimum of the final negative-ion fraction as the collision number $N \to \infty$ is $P_{\rm min}(F^-) = P_1/(P_1+P_2)$ and depends only on the projectile's velocity. However, this equation cannot be analytically solved. From numerical calculations, we obtain $P_{\rm min}(F^-) = 0.37$ at $v_0 = 0.05$ a.u., which is nearly consistent with the minimum value (0.39) obtained at a finite collision number ($N = 30$) for the same velocity. This value indicates that the equilibrium between the electron-loss and electron-capture processes is reached when it is insensitive to the effective number of binary collisions N. As the velocity increases, the collision time becomes short, and the number of collisions N is finite. Thus, the final negative-ion fraction is larger than $P_{\rm min}(F^-)$. In particular, the electron-capture process gradually begins to play an important role in the scattering process as the velocity increases and, as a result, the final negative-ion fraction increases after the inflection point. When $v > 0.1$ a.u., the magnitude of the transition zone ΔR may become so large that the Landau–Zener formula (Eq. (9)) will be substantially less effective.[42] Additionally, the effective interaction time $t_{\rm eff} \approx a_{\rm LiF}/(2v_{||})$ for a single collision is less than 38 a.u. This short time may also make the two-level crossing impossible and inefficient; thus, using the Landau–Zener model to describe electron loss is not valid.

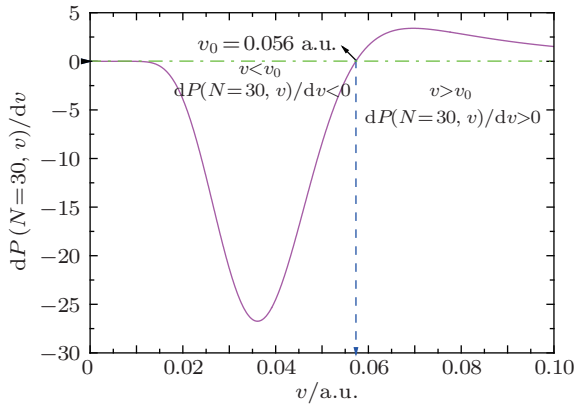


Fig. 4. (color online) $\mathrm{d}P(N=30,v)/\mathrm{d}v$ as a function of the negative projectile velocity v, where v_0 = 0.056 a.u. represents the zero point of $\mathrm{d}P(N=30,v)/\mathrm{d}v$.

4. Conclusion

The Demkov model has been successfully applied to describe negative-ion fractions at the low-velocity threshold, whereas electron loss to an insulating surface via negative-ion scattering is not well understood. Because of the substantial difficulty associated with performing full quantum calculations to investigate this problem, the Landau–Zener model is introduced in this work to treat the formed quasi-molecular ionic and covalent diabatic potential curves crossing at a small distance for the electron loss at surface cations. This model presents an analytical formula and can explain the electron-loss process for negative ions during grazing scattering on an insulator LiF(001) surface in the velocity range $v = 0$–0.1 a.u. The calculated results are in good agreement with the only available experimental data. It should be emphasized that the derived model and conclusions based on this low-velocity range can be generalized, even though they are based on the results of a specific case, i.e., a F^-–LiF(001) surface. We expect that this work will provide a fundamental basis for future detailed studies of electron loss during negative-ion surface scattering using both experimental and theoretical approaches.

References

[1] Souda R, Aizawa T, Hayami W, Otani S and Ishizawa Y 1990 *Phys. Rev. B* **42** 7761
[2] Souda R, Hayami W, Aizawa T, Otani S and Ishizawa Y 1992 *Phys. Rev. B* **45** 14358
[3] Souda R, Yamamoto K, Hayami W, Aizawa T and Ishizawa Y 1995 *Phys. Rev. B* **51** 4463
[4] Souda R, Hayami W, Aizawa T and Ishizawa Y 1991 *Phys. Rev. B* **43** 10062
[5] Auth C, Borisov A G and Winter H 1995 *Phys. Rev. Lett.* **75** 2292
[6] Maazouz M, Guillemot L, Lacombe S and Esaulov V A 1996 *Phys. Rev. Lett.* **77** 4265
[7] Ustaze S, Verucchi R, Lacombe S, Guillemot L and Esaulov V A 1997 *Phys. Rev. Lett.* **79** 3526
[8] Blauth D and Winter H 2011 *Nucl. Instr. and Meth. B* **269** 1175

[9] Auth C, Mertens A and Winter H 1998 *Phys. Rev. Lett.* **81** 4831
[10] Roncin P, Villette J, Atanas J P and Khemliche H 1999 *Phys. Rev. Lett.* **83** 864
[11] Chen L, Guo Y L, Jia J J, Zhang H Q, Cui Y, Shao J X, Yin Y Z, Qiu X Y, Lv X Y, Sun G Z, Wang J, Chen Y F, Xi F Y and Chen X M 2011 *Phys. Rev. A* **84** 032901
[12] Chen L, Ding B, Li Y, Qiu S L, Xiong F F, Zhou H, Guo Y L and Chen X M 2013 *Phys. Rev. A* **88** 044901
[13] Borisov A G, Sidis V and Winter H 1996 *Phys. Rev. Lett.* **77** 1893
[14] Borisov A G and Sidis V 1997 *Phys. Rev. B* **56** 10628
[15] Demkov Y N 1963 *Zh. Eksp Teor. Fiz.* **45** 195
[16] Demkov Y N 1964 *Sov. Phys. JETP* **18** 138
[17] Zhou H, Chen L, Feng D, Guo Y L, Ji M C, Wang G Y, Zhou W, Li Y, Zhao L and Chen X M 2012 *Phys. Rev. A* **85** 014901
[18] Borisov A G and Esaulov V A 2000 *J. Phys.: Condens. Matter* **12** R177
[19] Roncin P, Borisov A G, Khemliche H and Momeni A 2002 *Phys. Rev. Lett.* **89** 043201
[20] Zunger A and Freeman A J 1977 *Phys. Rev. B* **16** 2901
[21] Tessman J R, Kahn A H and Shockley W 1953 *Phys. Rev.* **92** 890
[22] Deutscher S A, Borisov A G and Sidis V 1999 *Phys. Rev. A* **59** 4446
[23] Tiwald P, Grafe S, Burgdorfer J and Wirtz L 2013 *Nucl. Instr. Meth. B* **317** 18–22
[24] Auth C, Mertens A, Winter H, Borisov A G and Sidis V 1998 *Phys. Rev. A* **57** 351
[25] Borisov A G, Sidis V and Winter H 1996 *Phys. Rev. Lett.* **77** 1893
[26] Winter H, Mertens A, Auth C and Borisov A G 1996 *Phys. Rev. A* **54** 2486
[27] Landau L D and Lifshitz E M *Quantum Mechanics (Nonrelativistic Theory)* (3rd Edn.)
[28] Rost J M 1999 *Phys. Rev. Lett.* **82** 1652
[29] Winter H, Auth C and Borisov A G 1996 *Nucl. Instr. Meth. B* **115** 133
[30] Page L J and Hygh E H 1970 *Phys. Rev. B* **1** 3472
[31] Ewing D H and Seitz F 1936 *Phys. Rev.* **50** 760
[32] Milgram A and Givens M P 1962 *Phys. Rev.* **125** 1506
[33] Mahan G D 1980 *Phys. Rev. B* **21** 4791
[34] Moore C 1949 *Atomic Energy Levels, Natl. Bur. Stand.* (U.S.) Circ. No 467 (U.S. GPO, Washington, DC, 1949) p. 8
[35] Zygelman B, Dalgarno A, Kimura M and Lane N F 1989 *Phys. Rev. A* **40** 2340
[36] West B W, Lane N F and Cohen J S 1982 *Phys. Rev. A* **26** 3164
[37] Zygelman B and Dalgarno A 1988 *Phys. Rev. A* **38** 1877
[38] Yan L L, Liu L, Wu Y, Qu Y Z, Wang J G and Buenker R J 2013 *Phys. Rev. A* **88** 012709
[39] Liu C H and Wang J G 2013 *Phys. Rev. A* **87** 042709
[40] Olson R E, Smith F T and Bauer E 1971 *Appl. Opt.* **10** 1848
[41] Olson R E 1972 *Phys. Rev. A* **6** 1822
[42] Bates D R 1960 *Proc. R. Soc. Lond. A* **257** 22
[43] Zener C 1932 *Proc. Roy. Soc. A* **137** 696
[44] Landau L D 1932 *Phys. Z. Sowjetunion* **2** 46
[45] Ostrovsky V N 1991 *J. Phys. B* **24** 4553
[46] Belyaev A K 2013 *Phys. Rev. A* **88** 052704